Journal of Materials Chemistry C

Accepted Manuscript

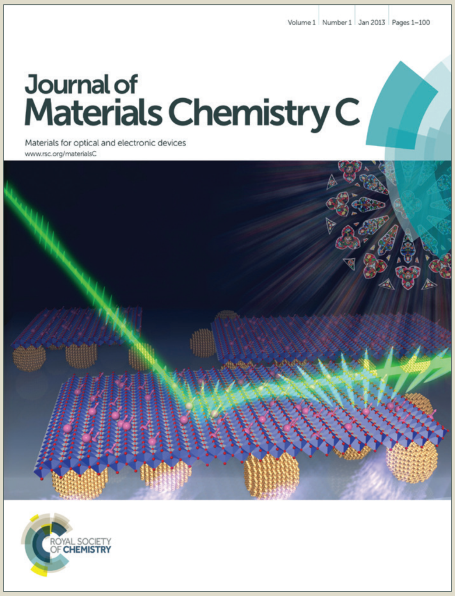

Volume 1 | Number 1 | Jan 2013 | Pages 1–100

Journal of Materials Chemistry C

Materials for optical and electronic devices

www.rsc.org/materialsC

ROYAL SOCIETY OF CHEMISTRY

ROYAL SOCIETY OF CHEMISTRY

www.rsc.org/materialsC

Journal of Materials Chemistry C

ARTICLE

Highly Sensitive Polymer Photodetectors with Broad Spectral Response Range from UV Light to NIR

Received 00th January 20xx,
Accepted 00th January 20xx

DOI: 10.1039/x0xx00000x

www.rsc.org/

Wenbin Wang,[a] Fujun Zhang,*[a] Lingliang Li,[a] Miao Zhang,[a] Qiaoshi An,[a] Jian Wang,[a] and Qianqian Sun[a]

Highly sensitive polymer photodetectors (PPDs) are successfully realized with broad spectral response range from UV light to near infrared region (NIR) based on P3HT:PTB7-Th:$PC_{71}BM$ as the active layer. The champion external quantum efficiency (EQE) values of PPDs with P3HT:$PC_{71}BM$ (100:1) as the active layer are 90,700% and 84,100% corresponding to 390 nm and 625 nm light illumination under ‑25 V bias, respectively. The spectral response range of PPDs is extended to NIR by doping narrow band gap polymer PTB7-Th into P3HT:$PC_{71}BM$ as the active layer. The champion EQE values of PPDs with P3HT:PTB7-Th:$PC_{71}BM$ (50:50:1) as the active layer are about 38,000% in the spectral range from 625 nm to 750 nm under ‑25 V bias. The realization of high EQE values of PPDs should be attributed to the three points: i) the rather weak dark current due to the relatively large hole injection barrier; ii) enhanced hole tunneling injection due to the interfacial band bending induced by trapped electrons in $PC_{71}BM$ near Al cathode; iii) efficient hole-only transport in the active layers with the rather low $PC_{71}BM$ content. The broad spectral response range is due to the contribution of PTB7-Th exciton dissociation on the number of trapped electrons in $PC_{71}BM$ near Al cathode.

1 Introduction

Polymer photodetectors (PPDs) have attracted more and more attention because of the rapid development of more excellent polymer semiconducting materials already used in polymer light emitting diodes and polymer solar cells.[1-4] The polymer semiconducting materials can provide many choices for obtaining highly sensitive PPDs due to their high absorption coefficient, adjustable energy level and band gap.[5-9] The highly sensitive photodetectors should have more circuiting charge carriers per absorbed photon by the active layer, i.e., the external quantum efficiency (EQE) in excess of 100%.[10-14] The photodiode type PPDs also exhibit low EQE values less than unity based on electron donor/acceptor (1:1, w/w) blend films as the active layers, which can be well explained from the limited photon harvesting efficiency, exciton dissociation efficiency, charge carrier transport and collection.[15-17] In fact, the mechanism of photodiode type PPDs is very similar with that of photovoltaic cells. Meanwhile, the working bias of photodiode type PPDs is relatively low due to the bicontinuous interpenetrating network for efficient charge carrier transport in the active layer, resulting in a relatively large dark current.[18] The optimized EQE values of photodiode type PPD are lower than 75% based on *p*-DTS$(FBTTh_2)_2$:PCBM (6:4, w/w) as the active layer.[19] For inorganic photodetectors or photomultiplier tube, the high EQE in excess of 100% can be easily realized based on impact ionization triggered by hot carriers, photoelectric emission effect or the secondary emission of electrons.[20,21] However, most of charge carriers in organic materials are localized in single molecule and intermolecular charge carrier transport occurs through thermal-activated hopping due to their disordered structure and large binding energy. Therefore, impact ionization and photoelectric emission effect can hardly be realized in organic materials due to their relative large binding energy.[22,23] Trap-assisted charge tunneling injection may open a window to obtain high EQE or photomultiplication (PM) phenomenon based on polymer or small molecule photodetectors. The mechanism of PM phenomenon in PPDs is that the photogenerated holes or electrons are trapped or blocked in the active layers, while opposite charge carries can continually pass through the active layers and are collected by the corresponding electrode.

In 1994, Hiramoto et al. first reported PM type organic photodetectors based on a simple structure Au/perylene/Au devices, the PM phenomenon is attributed to the strong electron injection from Au electrode to the perylene film assisted by the accumulation of photogenerated holes trapped near the Au/perylene interface.[24] A small amount of inorganic nanoparticles (CdTe) was doped into poly(3-hexylthiophene) (P3HT):[6,6]-phenyl-C_{61}-butyric acid methyl ester ($PC_{61}BM$) (1:1, w/w) blend solution to prepare the active layers of PPDs, and the PPDs exhibit a champion EQE of 8,000% at ‑4.5 V corresponding to 350 nm light illumination.[25] The high EQE value of photodetectors with P3HT:$PC_{61}BM$:CdTe as the active layer should be attributed to the enhance hole tunneling injection assisted by trapped electrons in CdTe nanoparticles. In fact, $PC_{61}BM$ in the blend films may not take positive effect on the performance of photodetectors due to the continuous electron transport channels formed by $PC_{61}BM$, resulting in a relatively large dark current. Huang's group also reported PM type UV-visible or UV photodetectors with

---

[a] Key Laboratory of Luminescence and Optical Information, Ministry of Education, Beijing Jiaotong University, Beijing, 100044, China Email: fjzhang@bjtu.edu.cn (Fujun),Tel: 0086-10-51684908

† Electronic Supplementary Information (ESI) available: [Light intensity spectrum of the monochromatic lights; EQE spectra of the PPDs; the detailed EQE, responsivity and detectivity values; the absorption spectra of blend films; the measured J_L and J_D of the PPDs.]. See DOI: 10.1039/x0xx00000x

nanocomposite active layers of ZnO nanoparticles blended with P3HT or PVK, ZnO nanoparticles was also considered as electron traps and polymers were used to harvest photon and form hole transport channels in the blend films.[10] The photodetectors with nanocomposite as the active layers exhibit an excellent performance under a relatively high bias of -9 V due to the efficient hole-only transport characteristics of the active layers. Dong et al. reported the highly sensitive photodetectors with broad spectral response range from UV to NIR by using PbS and ZnO quantum dots (QDs) doped into P3HT:PC$_{61}$BM (1:1, w/w) system as the active layer.[26] Chen and Chuang et al. also successfully realized PM type UV to NIR photodetectors based on NIR dye 4,5-benzoindotricarbocyanine (Ir-125) doped into P3HT:PC$_{61}$BM (1:1, w/w) as the active layer, exhibiting a peak EQE value of ~7,000% under -1.5 V bias at 510 nm light illumination, and the PM phenomenon is attributed to the enhanced hole injection assisted by trapped electrons in Ir-125 NIR dye.[12] Meanwhile, the spectral response of PPDs was further extended to longer wavelength (~1200 nm) through codoping of two NIR dyes (Ir-125 and Q-switch 1) into P3HT:PC$_{61}$BM (1:1, w/w) system.[27] The narrow band gap materials can be used as low energy photon harvesting centers to improve the sensitivity of photodetectors in the longer wavelength range. Recently, we proposed a smart strategy to obtain PM type PPDs with P3HT:[6,6]-phenyl-C$_{71}$-butyric acid methyl ester (PC$_{71}$BM) (100:1, w/w) as the active layer, the champion EQE value arrives to 16,700% under -19 V bias at 390 nm light illumination, which should be attributed to the enhanced hole tunneling injection assisted by trapped electrons in PC$_{71}$BM near Al cathode.[28] Therefore, the spectral response of PPDs may be extended to the long wavelength range by incorporating narrow band gap materials which can harvest low energy photon. This strategy has also been demonstrated as an effective method to improve spectral response range of solar cell by doping narrow bandgap material as the second electron donor, this kind of solar cells is called as ternary solar cells.[29-31] Narrow band gap polymer poly[4,8-bis(5-(2-ethylhexyl)thiophen-2-yl)benzo[1,2-b:4,5-b’]dit-hiophene-co-3-fluor-othieno[3,4-b]thiophene-2-carboxylate] (PTB7-Th) is a kind of high efficiency photovoltaic material due to its high photon harvesting ability in the long wavelength range.[32] Therefore, the polymer PTB7-Th may be one of the best candidates to improve the response of PPDs in the long wavelength range.

In this paper, a series of highly sensitive PM type PPDs with broad spectral response range from UV light to NIR were successfully obtained by using electron donor polymers P3HT and PTB7-Th, as well as electron acceptor PC$_{71}$BM as the active layer. For all the PPDs, the weight ratio of donors to acceptor is kept constant as 100:1(w/w), the only difference is the PTB7-Th doping ratio in donors. The EQE values of PPDs can be adjusted by changing PTB7-Th doping ratio in donors. The champion EQE values of PPDs are 90,700%, 84,100% and 38,000% corresponding to 390 nm, 625 nm and 750 nm light illumination under -25 V bias based on the active layers with different PTB7-Th doping ratio in donors. This strategy may provide a simple and effective method to obtain highly sensitive NIR PPDs by doping narrow band gap materials based on highly sensitive PPDs.

2 Experimental sections

The indium tin oxide (ITO) coated glass substrates with a sheet resistance of 15 Ω/square were sequentially cleaned by ultrasonic treatment in detergent, deionized water and ethanol. The cleaned ITO substrates were dried by nitrogen gas and treated by UV-ozone for 10 min to increase the work function of ITO surface. The solution of PEDOT:PSS was spin-coated onto the cleaned ITO substrates at a spin speed of 5000 rounds per minute (rpm) for 40 s. The PEDOT:PSS coated ITO substrates were baked at 120 ° C for 10 min. Polymer P3HT and PTB7-Th (purchased from Organtec Material Inc.) and PC$_{71}$BM (purchased from Luminescence Technology Corp.) were dissolved in 1,2-dichlorobenzene (*o*-DCB) to prepare 40mg/ml solutions, respectively. Then, the mixed solutions were prepared with different doping weight ratio of P3HT:PTB7-Th:PC$_{71}$BM from 100:0:1, 90:10:1, 70:30:1, 50:50:1, 30:70:1, 10:90:1 to 0:100:1. The mixed solutions were spin-coated onto PEDOT:PSS layers at 800 rpm for 30 s in high nitrogen-filled glove box, the thickness of the active layers is in the range from 280 nm to 300 nm. The 100 nm thick aluminum was thermally evaporated on the active layers in a high vacuum (10^{-4} pa) chamber. The active area of each device is about 3.8 mm^2, which is defined by the overlap of Al cathode and ITO anode.

The current density versus voltage (*J-V*) curves of PPDs were measured by a Keithley 2400 source meter under 390 nm, 625 nm or 750 nm light illumination with intensity of 13.0 μW/cm^2, 8.87 μW/cm^2 or 6.85 μW/cm^2, respectively. The used monochromatic light was provided by a 150 W xenon lamp coupled with a monochromator. The monochromatic light intensity and wavelength were monitored and calibrated by a Newport 818-UV power meter and an Acton SpectraPro 2150i CCD spectrometer. The absorption spectra of the active layers were measured by a SHINADZU UV-3101 PC spectrophotometer. The thickness of active layers was measured by a AMBIOS technology XP-2 stylus profilometer. All the measurements were carried out at room temperature in the ambient condition. Light intensity spectrum of the monochromatic lights through a monochromator was measured and is shown in **Fig. S1**. The chemical structures of used materials and schematic device structure are shown in **Fig. 1**.

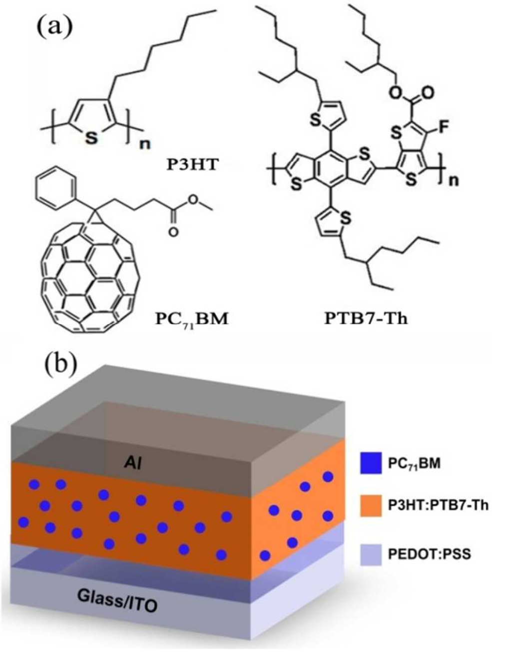

Fig. 1 (a) Molecular structures of organic materials P3HT, PTB7-Th, and PC$_{71}$BM; (b) Device structure of the PPDs.

3 Results and discussion

A series of PPDs with P3HT$_{100-x}$:PTB7-Th$_x$:PC$_{71}$BM$_1$ as the active layer were fabricated under the same conditions, the doping weight ratio of donors to acceptor is kept as 100:1 (w/w), the subscript x represents PTB7-Th doping ratio in donors. The EQE spectra of all PPDs were measured under different bias from −4 V to −25 V with an interval of 3 V. The EQE spectra of PPDs with P3HT$_{100}$:PC$_{71}$BM$_1$, P3HT$_{50}$:PTB7-Th$_{50}$:PC$_{71}$BM$_1$ or PTB7-Th$_{100}$:PC$_{71}$BM$_1$ as the active layer are shown in **Fig. 2 a-c**. And the EQE spectra of other PPDs with different PTB7-Th doping ratio in donors are shown in **Fig. S2**. The detailed EQE values of all PPDs at different reverse bias and light illumination are summarized and shown in **Table S1**.

It is apparent that the EQE values of PPDs with P3HT$_{100}$:PC$_{71}$BM$_1$ as the active layer are more than 100% in the spectral range from 350 nm to 700 nm when the reverse bias is larger than 4 V, as shown in **Fig. 2a**. The champion EQE values of PPDs with P3HT:PC$_{71}$BM as the active layer arrives to 90,700%, 84,100% and 850% under 390 nm, 625 nm and 750 nm light illumination and −25 V bias. There is a distinct dip between 490 nm and 570 nm in the EQE spectra, which well corresponds with the absorption spectrum of P3HT film, as shown in **Fig. S3a**. This phenomenon has been well demonstrated in our pervious paper,[33] which is attributed to the weakened trap-assisted hole tunneling injection resulting from the fewer trapped electrons in PC$_{71}$BM near Al cathode. It is known that only the PC$_{71}$BM near Al cathode can take into effect on interfacial band bending to assist hole tunneling injection from Al cathode onto the highest molecular occupied orbital (HOMO) of P3HT. There is also a distinct dip between 600 nm and 710 nm in the EQE spectra of PPDs with PTB7-Th$_{100}$:PC$_{71}$BM$_1$ as the active layer, as shown in **Fig. 2b**. The characteristics of EQE spectral dip well accord with the absorption spectral characteristics of PTB7-Th films, these fine characteristics are marked in **Fig. S3b**. This phenomenon can further confirm that the EQE spectral dip should be attributed to the decreased number of trapped electrons in PC$_{71}$BM near Al cathode when the PPDs are illuminated by the light in this spectral range. The trapped electrons should originate from donor (P3HT or PTB7-Th) excitons dissociation around the PC$_{71}$BM near Al cathode. It is known that much more photons have been harvested by the donor near ITO cathode when light is irradiated from ITO side, leading to the less generated excitons in donor and the fewer trapped electrons in PC$_{71}$BM near Al cathode. Therefore, the trap-assisted hole tunneling injection is weakened, resulting in the decreased EQE values in this spectral range.

Based on the EQE spectral characteristics of PPDs with P3HT:PC$_{71}$BM or PTB7-Th:PC$_{71}$BM as the active layer, it can be deduced that the dip in EQE spectra of PPDs should be formed due to the relatively strong absorption intensity of active layers in this spectral range. For the ternary P3HT$_{50}$:PTB7-Th$_{50}$:PC$_{71}$BM$_1$ blend films, there is a relatively broad absorption

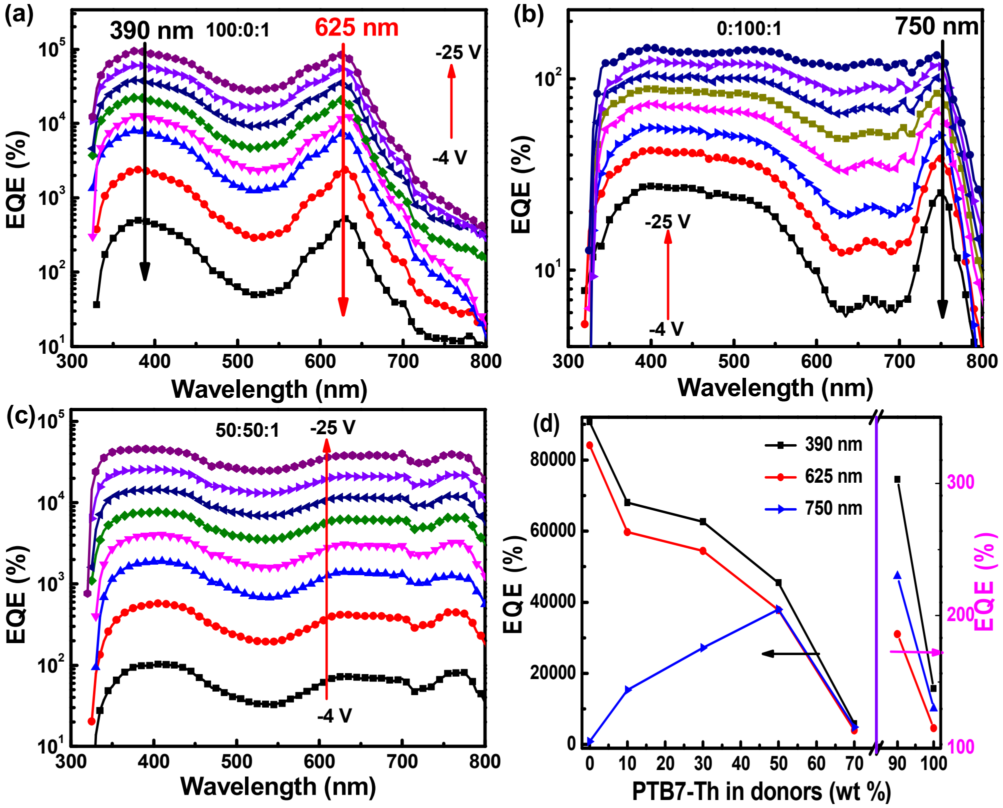

Fig. 2 EQE spectra of the PPDs under different bias from −4 V to −25 V with an interval of 3 V, (a) P3HT$_{100}$:PC$_{71}$BM$_1$; (b) PTB7-Th$_{100}$:PC$_{71}$BM$_1$; (c) P3HT$_{50}$:PTB7-Th$_{50}$:PC$_{71}$BM$_1$ as the active layer; (d) EQE values of the PPDs dependence on PTB7-Th doping ratio in donors at 390 nm, 625 nm and 750 nm light illumination under −25 V bias.

spectrum in the visible light range with two shoulder absorption peaks corresponding to the absorption peaks of P3HT and PTB7-Th. Therefore, the dip in EQE spectra of PPDs with $P3HT_{50}$:PTB7-Th_{50}:$PC_{71}BM_1$ as the active layer should be not very obvious, which is confirmed from the experimental results shown in **Fig. 2c**. The corresponding characteristics between EQE spectra of PPDs and absorption spectra of ternary blend films are one-to-one correspondence, as shown in **Fig. S3c**. Meanwhile, EQE values of all the PPDs are rapidly increased along with the increase of applied bias, which should be attributed to the enhanced charge carrier injection induced by interfacial band bending under higher bias and the improved hole transport in the active layers under high electric field. The phenomenon can be well explained by following equation:

$$\mathrm{EQE} = \frac{\chi\tau}{T} = \frac{\chi\tau\mu V}{L^2} \qquad (1)$$

where χ is the fraction of excitons that dissociated into trapped electrons and free holes, τ is the lifetime of trapped electron, T is the hole transport time, V is the applied bias, L is the active layer thickness, and μ is the field dependent hole carrier mobility.[34] It is apparent that the hole transport time (T) of passing through the whole active layer should be deceased under the higher applied bias, resulting in the increase of EQE values.

To more intuitive display the effect of PTB7-Th doping ratio in donors on EQE values, the EQE values of PPDs dependence on the PTB7-Th doping ratio in donors under –25 V bias are described in **Fig. 2d**. As we know, the major charge carrier in all the PPDs should be hole due to the rather low $PC_{71}BM$ content in the active layers. The EQE values of PPDs at 390 nm and 625 nm are monotonously decreased along with the increase of PTB7-Th doping ratio in donors, which may be attributed to the disrupted hole transport channels of P3HT by doping PTB7-Th in the active layers and the weakened hole tunneling injection from Al cathode into the active layers. However, the EQE values of the PPDs at 750 nm are increased from 850% to 38,000% and then decreased to 130% along with the increase of PTB7-Th doping ratio in donors. According to the EQE spectra of PPDs with PTB7-Th:$PC_{71}BM$ as the active layer (shown in **Fig. 2b**), the relatively large EQE values at 750 nm should be also attributed to the enhanced hole tunneling injection assisted by trapped electrons in $PC_{71}BM$ near Al cathode, the trapped electrons originate from exciton dissociation on PTB7-Th. The EQE values at 750 nm arrive to the maximum for the PPDs with $P3HT_{50}$:PTB7-Th_{50}:$PC_{71}BM_1$ as the active layer, which should be attributed to the best trade-off between hole tunneling injection and hole transport in this active layer. The trap-assisted hole tunneling injection is codetermined by i) the hole injection barrier from Al cathode onto the HOMO level of P3HT or PTB7-Th; ii) the trap depth corresponding to the lowest unoccupied molecular orbital (LUMO) levels difference between $PC_{71}BM$ and P3HT or between $PC_{71}BM$ and PTB7-Th. According to **Fig. 2a** and **2b**, the EQE values of PPDs with P3HT:$PC_{71}BM$ (100:1) as the active layer are much larger than those of PPDs with PTB7-Th:$PC_{71}BM$ (100:1) as the active layer under the same reverse bias. It is known that the hole mobility of PTB7-Th is better than that of P3HT,[35,36] which means that the trap-assisted hole tunneling injection (dependence on the number of trapped electrons in $PC_{71}BM$ near Al cathode, i.e. trap depth) should play a vital role on the EQE values of PPDs.

Based on the detailed characterization on the PM type PPDs, the responsivity (R) and detectivity (D*) values of PPDs dependence on photon wavelength were calculated under different bias, the responsivity and detectivity dependence on photon wavelength under -25 V and -10 V bias are shown in **Fig. 3** and **Fig. S4**, respectively. The detailed calculations of these values are expressed as the following:

$$\mathrm{EQE} = \frac{J_{ph} h\nu}{I_{in} e} \qquad (2)$$

$$\mathrm{R} = \frac{J_{ph}}{I_{in}} \qquad (3)$$

$$\mathrm{D}^* = \frac{R}{\sqrt{2eJ_d}} \qquad (4)$$

Here, J_{ph} is photocurrent density, $h\nu$ is photon energy, I_{in} is incident light intensity, J_d is dark current density and e is absolute value of electron charge.

It is known that the responsivity and detectivity of photodetectors strongly depend on the photon wavelength. The champion responsivity and detectivity values of PPDs with P3HT:PTB7-Th:$PC_{71}BM$ (100:0:1) as the active layers arrive to 284.9 A/W, 423.4 A/W, 5.2 A/W and 2.28×10^{13} Jones, 3.39×10^{13} Jones, 4.12×10^{11} Jones corresponding to 390 nm, 625 nm and 750 nm light illumination under -25 V bias, respectively. The champion responsivity and detectivity values of PPDs with P3HT:PTB7-Th:$PC_{71}BM$ (50:50:1) as the active layer arrive to 229.5 A/W and 1.91×10^{13} Jones at 750 nm light illumination under -25 V bias. The responsivity and detectivity improvement should be attributed to the contribution of PTB7-Th photogenerated exciton dissociation on the increased trapped electrons in $PC_{71}BM$ near Al cathode. Meanwhile, the relatively high responsivity and detectivity are also attributed to the rather low dark current, i) the relatively large hole injection barriers of 0.8 eV form Al cathode onto the HOMO of P3HT or 1.15 eV form Al cathode onto the HOMO of PTB7-Th; ii) the hole-only efficient transport in the active layers due to the rather low $PC_{71}BM$ content. Under illumination and bias, the interfacial band bending and band tilting of polymer materials will open the valve of hole tunneling injection, the injected holes will be

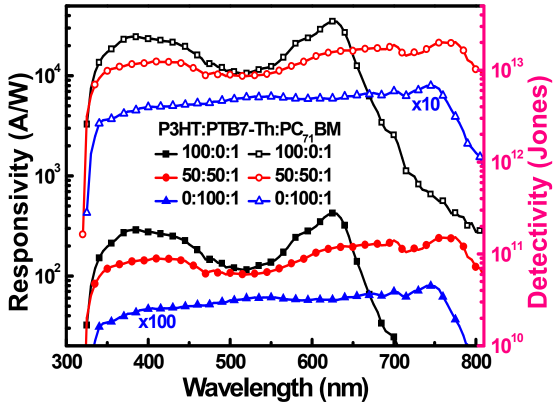

Fig. 3 The responsivity and detectivity dependence on the light wavelength of PPDs with different active layers under -25 V bias.

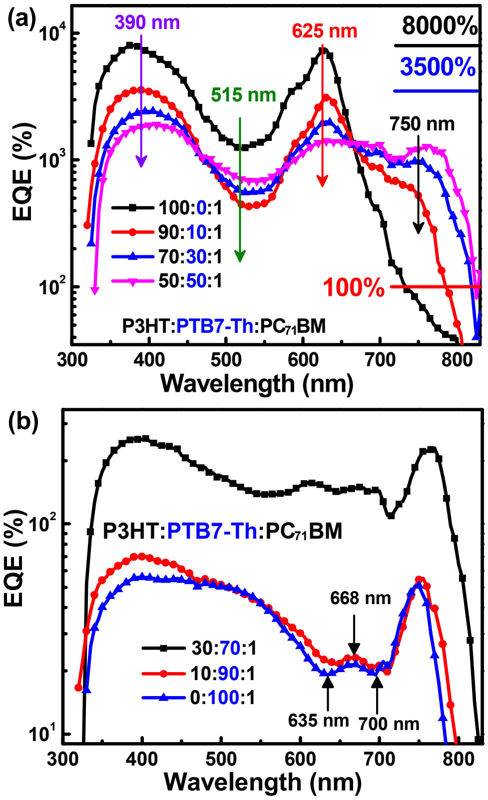

Fig. 4 (a) EQE spectra of PPDs with PTB7-Th doping ratio in donors from 0 to 50% under －10 V bias. (b) EQE spectra of PPDs with PTB7-Th doping ratio in donors from 70% to 100% under －10 V bias.

effectively transported in the active layers. Therefore, the performances of PM type PPDs exhibit a strong relationship dependence on the bias. The PM type PPDs also show good stability under high bias due to the single charge carrier transport characteristics of the active layers.

As we know, the energy levels of donors become more curved near the interfaces between the active layers and Al cathode when more electrons are trapped in $PC_{71}BM$ near Al cathode due to the stronger Coulomb field. To further investigate the effect of trap-assisted hole tunneling injection on the EQE values of PPDs, the EQE spectra of all PPDs with different PTB7-Th doping ratio in donors as the active layer are discussed under a relatively low bias (–10 V), as shown in **Fig. 4a** and **4b**. Under the low bias, the injected hole from Al cathode onto the HOMO level of donors is very difficult in the dark conditions due to the relatively large hole injection barriers of 0.8 eV for P3HT and 1.15 eV for PTB7-Th, which can be demonstrated from the current density-voltage (*J-V*) curves of all PPDs in dark, as shown in the **Fig. S5**.

It is apparent that the EQE values of PPDs are decreased along with the increase of PTB7-Th doping ratio in donors in the spectral range from 350 nm to 650 nm. However, the EQE values in the longer wavelength range (at 750 nm) are increased from ~76% to ~1,200% along with the PTB7-Th doping ratio up to 50 wt %, as shown in **Fig. 4a**. The EQE values of PPDs are lower than 100% in the whole spectral range when PTB7-Th doping weight ratios are more than 70% in donors, as shown in **Fig. 4b**. The dip in the EQE spectral range from 490 nm to 570 nm becomes less and less obvious along with the increase of PTB7-Th doping ratio in donors, which should be attributed to the decreased photon harvesting by P3HT in this range. However, the dip in the EQE spectral range from 600 nm to 710 nm becomes more and more obvious along with the increase of PTB7-Th doping ratio in donors. To further confirm the underlying reason for the dip in the EQE spectra, absorption spectra of the blend $P3HT_{100-x}$:$PTB7\text{-}Th_x$:$PC_{71}BM_1$ films were measured and are shown in **Fig. 5a**, the subscript is PTB7-Th doping weight ratio in donors, x=0, 10, 30, 50, 70, 90, 100. It is apparent that the dip in EQE spectra of each kind of PPDs well matches with the strong absorption peak of the active layer, respectively. There are two absorption peaks at 635 nm and 700 nm accompanying a valley at 668 nm in the absorption spectra of neat PTB7-Th films, these characteristics are finely projected in the EQE spectra of PPDs with PTB7-Th:$PC_{71}BM$ (100:1) as the active layer, as marked in **Fig. 4b**. In the EQE spectral dip ranges, the EQE values of PPDs with PTB7-Th:$PC_{71}BM$ (100:1) as the active layer are much smaller than those of PPDs with P3HT:$PC_{71}BM$ (100:1) as the active layer. Therefore, the trap-assisted hole tunneling injection of PPDs with PTB7-Th:$PC_{71}BM$ (100:1) as the active layer should be much weaker due to the fewer electrons trapped in $PC_{71}BM$ surrounded by PTB7-Th. The electron-trapped ability of $PC_{71}BM$ depends on the energy levels of donors surrounding it, which can be investigated from the energy levels of used materials.

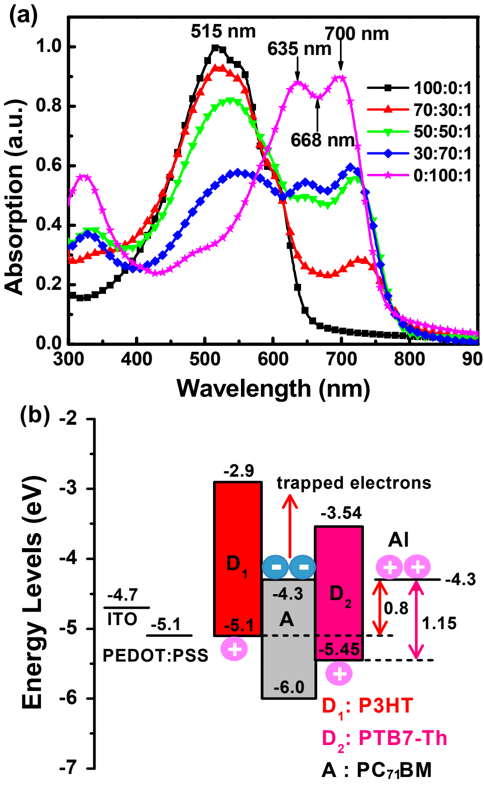

Fig. 5 (a) Absorption spectra of P3HT, PTB7-Th and their blend films with different PTB7-Th doping ratio in donors. (b) Schematic representation of the energy levels of used materials in the PPDs.

It is known that the photogenerated excitons on P3HT or PTB7-Th should be effectively dissociated into charge carriers at their interfaces with PC$_{71}$BM, the electrons will be trapped in PC$_{71}$BM molecules due to the absence of electron transport channels in the active layers with rather low PC$_{71}$BM content. The number of trapped electrons in PC$_{71}$BM should be determined by the LUMOs difference between PC$_{71}$BM and P3HT or PTB7-Th. The depth of electron traps is 0.76 eV or 1.4 eV corresponding to the PC$_{71}$BM surrounded by PTB7-Th or P3HT according to their energy levels, as shown in **Fig. 5b**. Therefore, more electrons can be trapped in PC$_{71}$BM surrounded by P3HT due to the deep traps (1.4 eV), leading to the more curved energy levels of P3HT near the interface between P3HT and Al cathode and the enhanced hole tunneling injection. However, relatively fewer electrons can be trapped in PC$_{71}$BM surrounded by PTB7-Th due to the shallow traps (0.76 eV), which will limit the trap-assisted hole tunneling injection. Meanwhile, the hole injection barrier is 0.8 eV or 1.15 eV from Al onto the HOMO of P3HT or PTB7-Th, respectively. The relatively large hole injection barrier from Al onto the HOMO of PTB7-Th is not conducive to the hole injection, which can be demonstrated from the *J-V* curve in dark conditions. For the PPDs with ternary materials as the active layer, the hole transport in the ternary films should be also limited due to the different HOMO levels of P3HT and PTB7-Th.

The current density-voltage (*J-V*) curves of all PPDs were measured in dark or under 625 nm light illumination with an intensity of 8.87 μ W/cm^2 or 750 nm light illumination with an intensity of 6.85 μ W/cm^2, respectively, as shown in **Fig. S5**. It is apparent that the dark current density of PPDs with PTB7-Th:PC$_{71}$BM (100:1) as the active layer is much less than that of PPDs with P3HT:PC$_{71}$BM (100:1) as the active layer. The photocurrent density (J_{ph}) curves of PPDs were calculated according to the *J-V* curves in dark and under light and are shown in **Fig. 6**. It is apparent that the J_{ph} of PPDs under 625 nm light illumination is decreased along with the increase of PTB7-Th doping ratio in donors, which well accords with the observed from EQE spectra of all PPDs. For the PPDs under 750 nm light illumination, the J_{ph} is increased and then decreased along with the increase of PTB7-Th doping ratio in donors. For the PPDs with relatively low PTB7-Th doping ratio in donors, P3HT can provide effective hole transport channels to improve the EQE values in the longer wavelength range. The J_{ph} of PPDs is decreased along with the increase of PTB7-Th doping ratio in donors, which should be attributed to the following points: i) fewer injected holes due to the large hole injection barriers of 1.15 eV from Al cathode onto the HOMO of PTB7-Th compared with that of 0.8 V from Al cathode onto the HOMO of P3HT; ii) the decreased interfacial contact area of P3HT/Al along with increase of PTB7-Th content in the active layers, iii) the limited hole transport in the blend films due to the different HOMO levels of P3HT and PTB7-Th, resulting in the increased charge carrier recombination in the active layers.

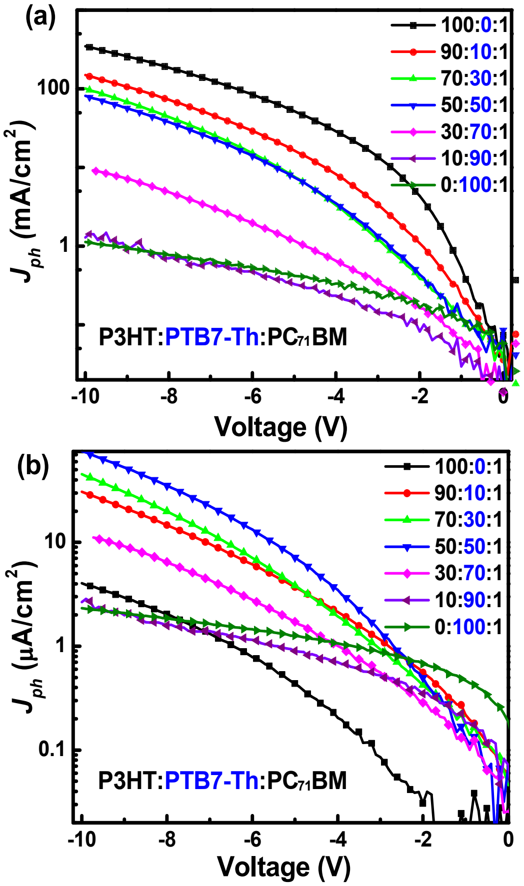

Fig. 6 J_{ph}-*V* curves of PPDs with different PTB7-Th doping ratio in donors under different light illumination. (a) 625 nm light illumination with an intensity of 8.87 μ W/cm^2. (b) 750 nm light illumination with an intensity of 6.85 μ W/cm^2.

To further clarify the working mechanism of PPDs with the active layers containing different PTB7-Th doping ratio, the transient photocurrent of PPDs was measured at -10 V under 625 nm or 750 nm light illumination which is modulated by an electronic shutter with a modulation period of 20 s, as shown in **Fig. 7**. The rise and fall processes of transient photocurrent become faster along with the increase of PTB7-Th doping ratio in donors. It is known that the transient photocurrent will come into saturation when the number of trapped electrons in PC$_{71}$BM arrives to a certain saturation state corresponding to a dynamic balance. In fact, there may be three kinds of electron traps of PC$_{71}$BM in the blend films, P3HT/PC$_{71}$BM/P3HT, PTB7-Th/PC$_{71}$BM/PTB7-Th and P3HT/PC$_{71}$BM/PTB7-Th. The shallow electron traps can be quickly filled in or emptied when the light is turned on or turned off. The number of trapped electrons in deep traps will take more time to arrive at the dynamic balance under the same conditions when light is turned on or turned off. As we can envisage, the number of traps formed by P3HT/PC$_{71}$BM/P3HT, P3HT/PC$_{71}$BM/PTB7-Th or PTB7-Th/PC$_{71}$BM/PTB7-Th are altered along with the increase of PTB7-Th doping ratio in donors. The rise and fall processes of transient photocurrent should be quicker due to the increased number of shallow traps formed by PTB7-Th/PC$_{71}$BM/PTB7-Th or P3HT/PC$_{71}$BM/PTB7-Th along with the increase of the PTB7-Th doping ratio in donors. The transient photocurrent, in turn, further demonstrates the PM phenomenon should be attributed to the enhanced hole tunneling injection assisted by trapped electrons in PC$_{71}$BM near Al cathode.

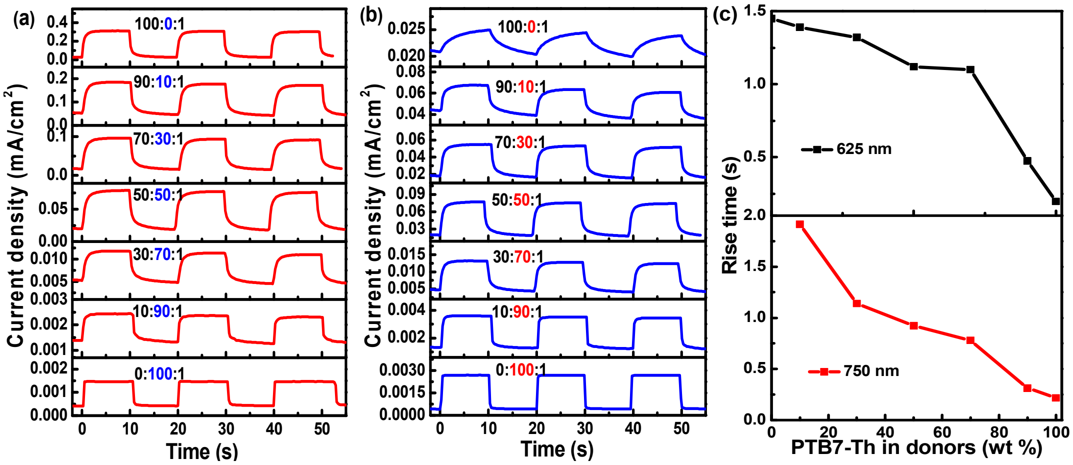

Fig. 7 Transient photocurrent of PPDs with P3HT$_{100-x}$:PTB7-Th$_x$:PC$_{71}$BM$_1$ as the active layer under −10 V bias, (a) 625 nm light illumination with an intensity of 8.87 μW/cm^2. (b) 750 nm light illumination with an intensity of 6.85 μW/cm^2. (c) Rise time (defined as the time required for the response change from 10% to 90% of the peak value of the PPDs) of the PPDs dependence on PTB7-Th doping ratio in donors at 625 nm and 750 nm light illumination under −10 V bias.

Another interesting phenomenon is that transient photocurrent of the PPDs with P3HT:PC$_{71}$BM (100:1) as the active layer exhibits very slow rise and fall processes under 750 nm light illumination, as shown in **Fig. 7b**. This phenomenon can also be well understood from the number of trapped electrons in PC$_{71}$BM surrounded by P3HT near Al cathode under 750 nm light illumination. According to the absorption spectrum of the blend P3HT:PC$_{71}$BM film (**Fig. 5a**), the blend film exhibits rather weak light absorption at 700 nm. It means that the deeper electron traps (P3HT/PC$_{71}$BM/P3HT) are hardly be filled in under 750 nm light illumination. Therefore, transient photocurrent of PPDs with P3HT:PC$_{71}$BM (100:1) as the active layer shows the rather slow rise and fall processes under 750 nm light illumination. This phenomenon further demonstrates the working mechanism of PM type PPDs based on the enhanced hole tunneling injection under the assistance of trapped electrons in PC$_{71}$BM near Al electrode. The accelerated response speed of PM type PPDs should be one of key issues for its potential application, which may be resolved by controlling the photogenerated electron distribution in the active layers.

4 Conclusions

In summary, we successfully developed highly sensitive PPDs with broad spectral response range from UV to NIR by using P3HT$_{100-x}$:PTB7-Th$_x$:PC$_{71}$BM$_1$ as the active layer. The champion EQE values of PPDs with P3HT:PTB7-Th:PC$_{71}$BM (100:0:1) as the active layer are 90,700% and 84,100% corresponding to 390 nm and 625 nm light illumination under −25 V bias, respectively. The PM phenomenon should be attributed to the enhanced hole tunneling injection assisted by trapped electrons in PC$_{71}$BM near Al cathode. High EQE values of PPDs are extended to NIR by doping narrow band gap polymer PTB7-Th into P3HT:PC$_{71}$BM. The champion EQE values of the PPDs with P3HT$_{50}$:PTB7-Th$_{50}$:PC$_{71}$BM$_1$ are about 38,000% in the spectral range from 625 nm to 750 nm under −25 V bias. This strategy may provide an effective method for organic photodetectors to achieve PM phenomenon with broad spectral response based on the trap-assisted charge tunneling injection.

Acknowledgements

This work was supported by Fundamental Research Funds for the Central Universities (2014JBZ017), National Natural Science Foundation of China (61377029).

Notes and references

1. H. L. Dong, H. F. Zhu, Q. Meng, X. Gong and W. P. Hu, *Chem. Soc. Rev.*, 2012, **41**, 1754-1808.
2. J. Wang, F. J. Zhang, J. Zhang, W. H. Tang, A. W. Tang, H. S. Peng, Z. Xu, F. Teng and Y. S. Wang, *J. Photoch. Photobio. C*, 2013, **17**, 69-104.
3. Z. H. Chen, P. Cai, J. W. Chen, X. C. Liu, L. J. Zhang, L. F. Lan, J. B. Peng, Y. G. Ma and Y. Cao, *Adv. Mater.*, 2014, **26**, 2586-2591.
4. F. J. Zhang, X. W. Xu, W. H. Tang, J. Zhang, Z. L. Zhuo, J. Wang, J. Wang, Z. Xu and Y. S. Wang, *Sol. Energy Mater. Sol. Cells*, 2011, **95**, 1785-1799.
5. D. Z. Yang and D. G. Ma, *J. Mater. Chem. C*, 2013, **1**, 2054.
6. Z. W. Jin and J. Z. Wang, *J. Mater. Chem. C*, 2013, **1**, 7996.
7. K. J. Baeg, M. Binda, D. Natali, M. Caironi and Y. Y. Noh, *Adv. Mater.*, 2013, **25**, 4267-4295.
8. J. Qi, L. Ni, D. Z. Yang, X. K. Zhou, W. Q. Qiao, M. Li, D. G. Ma and Z. Y. Wang, *J. Mater. Chem. C*, 2014, **2**, 2431.
9. T. K. An, C. E. Park and D. S. Chung, *Appl. Phys. Lett.*, 2013, **102**, 193306.
10. F. W. Guo, B. Yang, Y. B. Yuan, Z. G. Xiao, Q. F. Dong, Y. Bi and J. S. Huang, *Nat. Nanotech.*, 2012, **7**, 798-802.
11. S. Park, B. T. Lim, B. Kim, H. J. Son and D. S. Chung, *Sci. Rep.*, 2014, **4**, 5482.
12. F. C. Chen, S. C. Chien and G. L. Cious, *Appl. Phys. Lett.*, 2010, **97**, 103301.
13. J. S. Huang and Y. Yang, *Appl. Phys. Lett.*, 2007, **91**, 203505.

14. I. H. Campbell and B. K. Crone, *Appl. Phys. Lett.*, 2009, **95**, 263302.
15. H. W. Lin, S. Y. Ku, H. C. Su, C. W. Huang, Y. T. Lin, K. T. Wong and C. C.Wu, *Adv. Mater.*, 2005, **17**, 2489-2493.
16. L. L. Li, F. J. Zhang, Q. S. An, Z. X. Wang, J. Wang, A. W. Tang, H. S. Peng, Z. Xu and Y. S. Wang, *Opt. Lett.*, 2013, **38**, 3823-3826.
17. Y. Yao, Y. Liang, V. Shrotriya, S. Xiao, L. Yu and Y. Yang, *Adv. Mater.*, 2007, **19**, 3979.
18. C. H. Cui, W. Y. Wong and Y. F. Li, *Energy Environ. Sci.*, 2014, **7**, 2276-2284.
19. I. K. Kim, B. N. Pal, M. Ullah, P. L. Burn, S. C. Lo, P. Meredith and E. B. Namdas, *Adv. Optical Mater.*, 2014, **3**, 50-56.
20. S. M. Sze, *Physics of Semiconductor Devices*, wiley, London, 1981.
21. A. Nevet, A. Hayat and M. Orenstein, *Opt. Lett.*, 2011, **36**, 725-727.
22. J. Reynaert, V. I. Arkhipov, P. Heremans and J. Poortmans, *Adv. Funct. Mater.*, 2006, **16**, 784-790.
23. L. A. A. Pettersson, L. S. Roman and O. Inganäs, *J. Appl. Phys.*, 2001, **89**, 5564-5569.
24. M. Hiramoto, T. Imahigashi and M. Yokoyama, *Appl. Phys. Lett.*, 1994, **64**, 187-189.
25. H. Y. Chen, M. K. F. Lo, G. W. Yang, H. G. Monbouquette and Y. Yang, *Nat. Nanotech.*, 2008, **3**, 543-547.
26. R. Dong, C. Bi, Q. F. Dong, F. W. Guo, Y. B. Yuan, Y. J. Fang, Z. G. Xiao and J. S. Huang, *Adv. Opt. Mater.*, 2014, **2**, 549-554.
27. S. T. Chuang, S. C. Chien and F. C. Chen, *Appl. Phys. Lett.*, 2012, **100**, 013309.
28. L. L. Li, F. J. Zhang, J. Wang, Q. S. An, Q. Q. Sun, W. B. Wang, J. Zhang and F.Teng, *Sci. Rep.*, 2015, **5**, 9181.
29. T. Ameri, P. Khoram, J. Min and C. J. Brabec, *Adv. Mater.*, 2013, **25**, 4245-4266.
30. Q. S. An, F. J. Zhang, L. L. Li, J. Wang, J. Zhang, L. Y. Zhou and W. H. Tang, *ACS Appl. Mater. Interfaces*, 2014, **6**, 6537-6544.
31. A. Kokil, A. M. Poe, Y. Bae, A. M. Della Pelle, P. J. Homnick, P. M. Lahti, J. Kumar and S. Thayumanavan, *ACS Appl. Mater. Interfaces*, 2014, **6**, 9920-9924.
32. S. H. Liao, H. J. Jhuo, Y. S. Cheng and S. A. Chen, *Adv. Mater.*, 2013, **25**, 4766-4771.
33. L. L. Li, F. J. Zhang, W. B. Wang, Q. S. An, J. Wang, Q. Q. Sun and M. Zhang, *ACS Appl. Mater. Interfaces*, 2015, **7**, 5890-5897.
34. I. H. Campbell and B. K. Crone, *J. Appl. Phys.*, 2007, **101**, 024502.
35. J. Kim, G. Kim, T. K. Kim, S. Kwon, H. Back, J. Lee, S. H. Lee, H. Kang and K. Lee, *J. Mater. Chem. A*, 2014, **2**, 17291-17296.
36. V. D. Mihailetchi, H. X. Xie, B. de. Boer, L. J. A. Koster and P. W. M. Blom, *Adv. Funct. Mater.*, 2006, **16**, 699-708.